Directed Rotations of Single Porphyrin Molecules Controlled by Localized Force Spectroscopy

Rémy Pawlak,[†,*] Sweetlana Fremy,[†] Shigeki Kawai,[†] Thilo Glatzel,[†] Hongjuan Fang,[‡] Leslie-Anne Fendt,[‡] François Diederich,[‡] and Ernst Meyer[†]

[†]Department of Physics, University of Basel, Klingelbergstrasse 82, 4056 Basel, Switzerland and [‡]Laboratory of Organic Chemistry, Department of Chemistry and Applied Biosciences, ETH Zürich, Honggerberg, HCI, 8093 Zürich, Switzerland

ABSTRACT

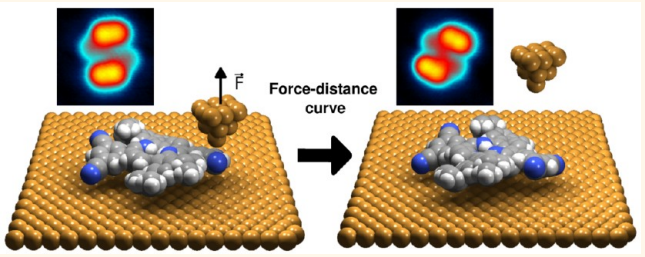

Directed molecular repositioning is a key step toward the build up of molecular machines. To artificially generate and control the motion of molecules on a surface, excitations by light, chemical, or electrical energy have been demonstrated. Here, the application of local mechanical forces is implemented to achieve directed rotations of molecules. Three-dimensional force spectroscopy with sub-Ångström precision is used to characterize porphyrin derivatives with peripheral carbonitrile groups. Extremely small areas on these molecules ($\approx$100 $\times$ 100 pm^2) are revealed which can be used to control rotations. In response to the local mechanical forces, the molecular structure elastically deforms and then changes its conformation, which leads to its rotation. Depending on the selection of one of four submolecular areas, the molecule is either rotated clockwise or counterclockwise.

KEYWORDS: porphyrin molecule · manipulation · scanning tunneling microscopy · noncontact atomic force microscopy · three-dimensional force spectroscopy

Molecular diffusion plays a decisive role in biological systems, self-assembly processes, and chemical reactions. In the spirit of developing molecular nanomachines, many attempts have been made to artificially control this diffusion mechanism by powering molecules with light,[1] chemical reactions,[2] or electric fields.[3,4] However, although parameters like the intrinsic elasticity of the molecular structure or its bonding to the surface are crucial in all diffusive processes, experimental evidence of their impact at the molecular scale is rather rare.[5] To investigate these processes at this spatial limit, scanning probe microscopy techniques[6,7] are powerful tools since they enable high-resolution imaging of surfaces in real-space as well as tip-induced repositioning down to the atomic level. Scanning tunneling microscopy (STM) has been the first technique to successfully demonstrate the manipulation of adsorbed atoms[8,9] and molecules.[10,11] However, STM probes the local electronic density of the molecules, and although efficient manipulation processes have been developed,[5,12,13] a straightforward determination of their elasticity is impossible. Since the first systematic achievement of atomic resolution in 1995, noncontact atomic force microscopy (nc-AFM) has become an efficient tool for surface science investigations.[14] This technique, based on the detection of the resonance frequency shift Δf of an oscillating cantilever, detects the interaction force gradients between a tip and a surface and is thus suitable to investigate mechanical properties of nanostructures at the atomic scale.[15] Similar to STM experiments, vertical and lateral tip-induced repositioning of atoms[16−18] or molecules[19−21] has been demonstrated. Furthermore, recent progress has also drastically increased the short-range force sensitivity[23,24] and allows one to observe the chemical structure of molecules[25−28] and chemically identify atomic species,[22] which makes nc-AFM one of the most powerful techniques for atomic-scale manipulations.

In this work, we investigate the mechanical properties of free-based porphyrins confined on Cu(111) in the saddle conformation *via* 3D spectroscopic measurements of force and current with sub-Ångström precision. We report a reliable method, which consists of creating Cu-coordinated bonds between specific end groups of the molecules and the AFM tip, to apply

* Address correspondence to remy.pawlak@unibas.ch.

Received for review April 23, 2012 and accepted June 3, 2012.

Published online June 03, 2012
10.1021/nn301774d

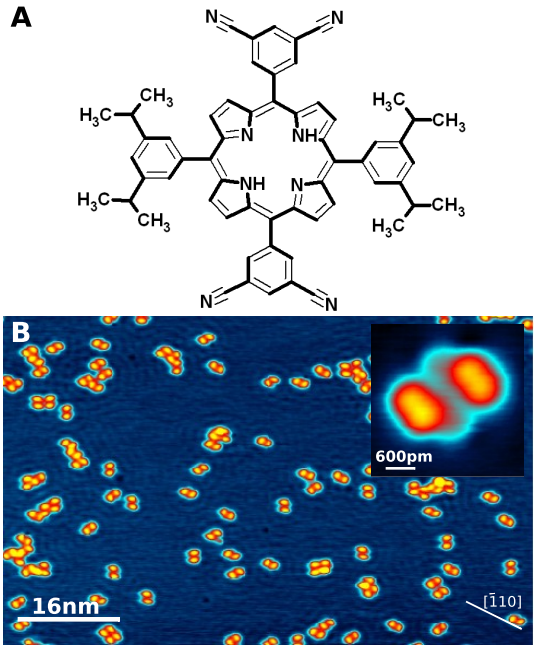

Figure 1. (A) Chemical structure of the free-base porphyrin equipped with two *meso*-(3,5-dicyanophenyl) and two *meso*-(3,5-di-*tert*-butylphenyl) rings. (B) Constant-current STM image of porphyrins adsorbed on Cu(111) in the saddle-shape geometry (I_t = 25 pA, V_{tip} = +500 mV, no resonant oscillation).

site-dependent vertical forces on the molecular structure. In this way, localized deformation is controlled which leads to a mechanically induced rotation of the molecules in a reproducible manner.

RESULTS AND DISCUSSION

Adsorption of the H_2TBCPP Molecule on Cu(111). The chemical structure of the H_2TBCPP molecule is depicted in Figure 1A and consists of a free-base porphyrin core functionalized with two *meso*-(3,5-dicyanophenyl) and two *meso*-(3,5-di-*tert*-butylphenyl) peripheral rings.[29] In the past, carbonitrile groups (CN) have proven their capacity for organometallic complexation,[30] which has been used to control the build up of self-assembled molecular systems[31] or as an anchoring point *via* a charge transfer on metallic substrates.[32] On insulating surfaces, its strong dipolar moment also enhances the molecular adsorption.[19,33−35]

Typical constant-current STM images after deposition on Cu(111) show that all isolated molecules are aligned along the [001] surface direction (Figure 1B). As shown in the inset of Figure 1B, porphyrin molecules imaged by STM appear with two bright spots and two darker lobes corresponding to the two di-*tert*-butylphenyl and the dicyanophenyl side groups, respectively. On the surface, a conformational change, the so-called saddle geometry,[36] is observed and consists of a rotation of the phenyl side group out of the surface plane as well as a lateral tilt of these legs in the plane of the porphyrin core. Furthermore, a bending of the two pyrrolic units of the porphyrin core upward and downward of 20−30° occurs which is due to a steric hindrance between adjacent legs.[36] The C_{2v} symmetry of the molecules is reduced to C_2 after adsorption, and two enantiomers are observed on the surface. Moreover, since free-base porphyrins only functionalized with di-*tert*-butylphenyl groups do not show a saddle conformation on Cu(111),[37] the molecule−substrate interaction might be essentially driven by the dicyanophenyl side groups interacting with the substrate, leading to the saddle conformation.

Carbonitrile Group Recognition. To investigate the mechanical properties of the molecule structure, systematic 3D spectroscopic measurement was conducted above single molecules (Figure 2; see also Methods). The closest recorded $I_t(x,y)$ map and a vertical cross section of $I_t(x,z)$ taken along the AA′ axis (Figure 2A,B) reveal the local electronic density of the molecule and recall the shape observed by STM. In contrast, the closest $\Delta f(x,y)$ map and the $\Delta f(x,z)$ cross section (Figure 2C,D) show the molecule mainly as a dark protrusion. Since only long-range attractive interaction forces are inducing the molecular contrast at this tip−molecule distance, the achievement of resolution of the chemical structure cannot be expected.[15,25] However, the periphery of the molecule shows four localized peaks with more positive Δf (≈30 Hz) corresponding to the exact location of the N atoms of the dicyanophenyl side groups. Regarding the $\Delta f(x,z)$ cross section, Δf remains positive during the tip retraction and reveals different z decay lengths depending on the considered N atom.

Typical $I_t(z)$ and $\Delta f(z)$ curves at a N atom position are plotted in Figure 2E,F, respectively. Both show a hysteresis loop with an abrupt variation (transition 1-2 in Figure 2F) in the conductivity (≈50 pA) as well as in the frequency shift during approach (≈30 Hz), an observation that we attribute to a junction formed between a N atom of the molecule and the Cu-terminated tip. By integrating the $\Delta f(z)$ curve along the z direction up to 1, the extracted vertical force F_z required to create this bond is found to be about −180 pN. Knowing that, for small oscillation amplitudes, the tip−sample stiffness is $k_{ts} = -2k\Delta f/f_0$ (with f_0 being the resonance frequency and k the tuning fork stiffness), the extracted k_{ts} at 1 in Figure 2F is typically 1.5 N/m and corresponds to the stiffness of the tip−molecule junction. This connection, arising from site-dependent long-range forces, is induced by a N···Cu coordination interaction formed between Cu adatoms at the tip apex and one N atom of the CN group. While the tip is being retracted (region 2-3), this link is sufficiently strong to lead to a vertical lift of the CN group, as illustrated in the inset of Figure 2F. On one hand, the conductivity is decreased in this region as a consequence of the CN end group lift and its disconnection from the substrate.[38] On the other hand, the Δf signal jumps to more positive values,

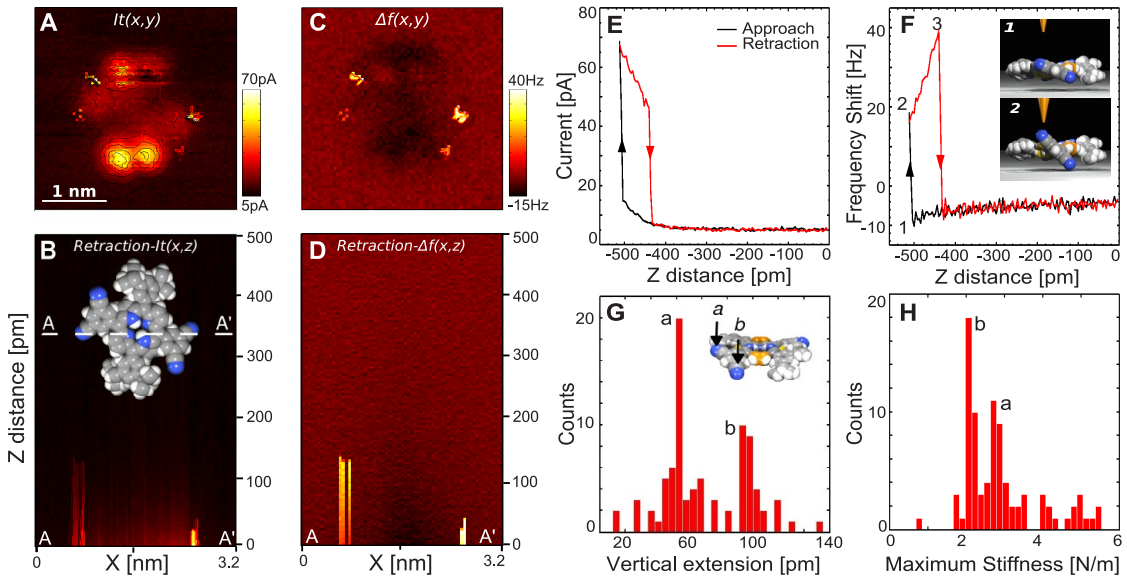

Figure 2. (A) $I_t(x,y)$ map of a 3D-DFS data set extracted at the closest tip−sample distance above a single porphyrin, and (B) $I_t(x,z)$ cross section taken along the AA′ axis (see dashed line inset of (B)). (C,D) Closest $\Delta f(x,y)$ map and $\Delta f(x,z)$ cross section taken along AA′. Four spots of positive frequency shift are identified with sub-Ångström precision in the $\Delta f(x,y)$ map at N atom locations of the dicyanophenyl side groups. (E,F) Individual approach−retract $I_t(z)$ and $\Delta f(z)$ curves taken at the N atom position showing a hysteresis process. A tip−molecule junction is formed during approach (transition 1-2), which allows the lift of the dicyanophenyl leg during retraction (region 2-3) as illustrated in the inset. (G,H) Vertical extension of the N atoms out of the surface plane and the maximum tip−sample stiffness during the switching process. In both graphs, two peaks marked *a* and *b* are distinguishable as a consequence of the asymmetry of the dicyanophenyl leg in the saddle conformation (V_{tip} = +300 μV, A = 50 pm).

which suggests a strong tip−molecule interaction.[39] Since the curve is not continuous in this region, the extraction of the total vertical force is not possible anymore. Although Δf is positive, we do not think that the actual vertical force corresponds to repulsive forces, but rather that the tip−molecule interaction forces are in the short-range attractive force regime since a coordination bond is formed between the tip and the porphyrin leg. We assume that the abrupt jump of Δf is the consequence of the drastic tip modification while attaching to the molecule. When the relative tip−sample distance becomes larger (≈100 pm), the $\Delta f(z)$ and $I_t(z)$ curves jump back to their initial shape (3 in Figure 2F) and coincide perfectly with the approach curve. Thus the manipulated side group recovers its initial state in the saddle conformation, which was systematically confirmed with STM images afterward. This vertical switching is reversible and always observed regardless of the considered molecule and the targeted N atom.

Figure 2G,H describes a statistical analysis of the *z* extension length and the maximum tip−sample stiffness recorded during the switching process. To obtain this, we have systematically collected several data sets for each manipulation process, such as the length of the hysteresis loop and the maximum $\Delta f(z)$ (region 2-3 Figure 2E), and then extracted the maximum tip−sample stiffness. These histograms reveal two peaks each, marked *a* and *b*, corresponding to two typical lifts of the porphyrin leg along *z* (≈50 and ≈90 pm) and two distinct tip−sample stiffnesses (≈2 and ≈2.9 N/m). Due to the nonplanarity of the phenyl leg in the saddle conformation (inset of Figure 2G), the actual height of one N atom slightly differs from the adjacent one as well as their interaction with the Cu(111) surface, which leads to these two significant responses during the manipulation.

Directed Motion Depending on the Selected CN Group. The achievement of mechanically induced repositioning of molecules requires an accurate control of the tip−molecule junction with a single CN end group. For this, we defined an area of 100 × 100 pm^2 above one N atom of a dicyanophenyl side group in accordance with the $\Delta f(z)$ maps (Figure 2C) and acquired several distance-dependent curves (from 1 to 30 *z* curves) at one of these locations.[40] Using this method, we found that a planar rotation of the molecule is reliably induced on the surface *via* a single *z* spectroscopic curve when the tip is slightly further approached compared to Figure 4F (≈20 pm). Since the molecule is equipped with two dicyanophenyl side groups, four N atoms in total (blue marks in Figure 3A) can be used for the manipulation. Furthermore, to avoid lateral shifts due to drift or piezo creep and to ensure successful reach to the N site during the whole experiments, atom-tracked tip positioning was activated above one *tert*-butyl group between two spectroscopic curves.[40] Figure 3B−E describes successive manipulations of single molecules depending on the selected N atom. Although the manipulation always consists of

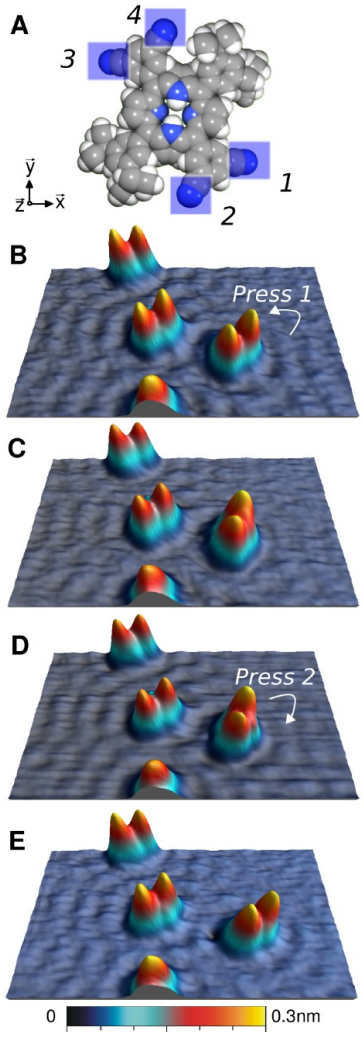

Figure 3. (A) Schematics of the H_2TBCPP in the saddle-shaped conformation. Four N atoms marked 1, 2, 3, and 4 can be targeted with *z* spectroscopic curves for inducing the rotation of the whole molecule. (B–E) Constant-current STM images of the same area showing successive manipulations of H_2TBCPP depending on the selected N atoms (marked on the images). STM parameters: V_{tip} = +60 mV, I_t = 30 pA. Spectroscopic curves: A = 50 pm, V_{tip} = +300 μV.

a 60° rotation, the direction with respect to the initial orientation is mediated by the N atom used for applying the localized deformation. Considering Figure 3A, we found that clockwise rotations are induced by attaching the tip to the N sites 2 and 4, whereas counterclockwise rotations arise from the sites 1 and 3, regardless of the chosen enantiomer. Our method has been tested with many molecules (≈65) and is readily induced (≈47 molecules). Unknown conformations or the unexpected termination of the tip apex with the molecule are sometimes observed (≈20 and ≈5%, respectively) that we considered as unsuccessful events. In total, the rotational process was successfully induced with a rate of about 75%, where molecules remain in the saddle conformation after motion.

Insights into the Manipulation Mechanism. Figure 4 shows typical spectroscopic data of simultaneously recorded $\Delta f(z)$ and dissipated energy $E_z(z)$ values while a rotation occurs. A successful manipulation (Figure 4A) always gives a larger hysteresis loop in $\Delta f(z)$ of ≈200 pm (Figure 4B) and a relevant peak in the dissipation channel (Figure 4C). Since the variation of current is small (≈40 pA, V_t = 300 μV), we conclude that the manipulation activation is not electrically driven, contrary to previous results,[3,4] but a consequence of the localized deformation applied to the molecule during tip retraction. Regarding the data shown in Figure 2, where no rotation is induced, the manipulation is obtained when the tip is slightly approached closer to the CN end group (from ≈20 to 50 pm) compared to the tip–sample separation, where the junction is first created (marked by 1 in Figure 4B). We also think that the number of *z* spectroscopic curves required to activate the rotation (typically 1 to 30) is related to the probability to create a "good" tip–molecule binding susceptible to induce the manipulation. The $\Delta f(z)$ curve in Figure 4B shows a similar behavior in the transition 1-2 compared to that in Figure 2F, where an abrupt jump is observed after creation of the tip–molecule binding as well as the increase of the Δf values while retracting the tip. Note also that the *z* length of this region (≈50 pm) is also in good agreement with the ones obtained in Figure 2. The major change of this $\Delta f(z)$ curve consists of an extension of the hysteresis loop (≈150 pm) accompanied by a change of the Δf gradient (transition 2-3, colored gray, compared to the transition 1-2). To explain this, we think that the manipulation process enters a regime where the lift of the CN group linked to the oscillating tip imposes the lateral displacement of the adjacent CN group in contact with the copper substrate, up to the vertical repositioning of the dicyanophenyl leg compared to the surface (Figure 4E,F). The second CN group interacting with the surface is thus partially decoordinated and slides from one copper atomic site to another (Figure 4F). We attribute the gradual increase of the $\Delta f(z)$ in the transition 2-3 to this unstable configuration of the junction at the surface, which induces stochastic changes of the tip–sample interaction.[39,41]

This assumption is further corroborated by the corresponding dissipated energy between the tip and the molecule during the process (Figure 4C), which always shows a peak when the rotation is induced. A statistical distribution of the dissipation maxima obtained over 47 manipulations regardless of the targeted CN groups is shown in Figure 4D, where two peaks clearly appear around 20 and 55 meV/cycle (fitted curves in Figure 4D). Here again, the relative instability of the tip–sample junction in the configuration "leg standing up" gives rise to a strong increase of the dissipation energy.[41] The extraction of quantitative dissipation energies from the spectroscopic data is thus complex since the magnitude of the dissipation might be modified by the oscillation amplitude of the

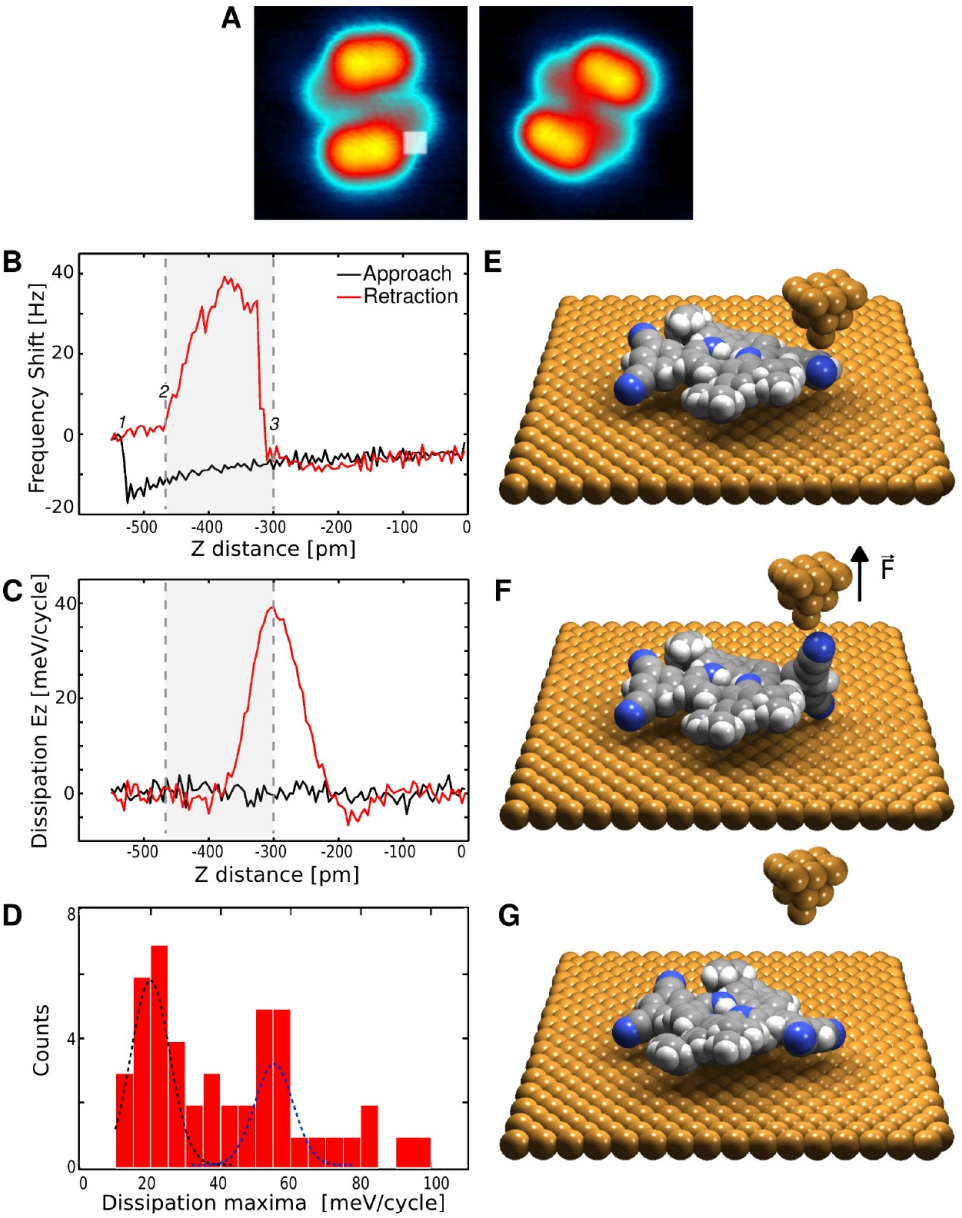

Figure 4. (A) Successive STM images showing a single rotation of the H_2TBCPP; the white area shows the position of the *z* spectroscopic curve (I_t = 25 pA, V_{tip} = 60 mV). Typical (B) $\Delta f(z)$ and (C) dissipation signal $E(z)$ curves leading to the rotation (V_{tip} = 300 μV, A = 50 pm). (D) Statistic of the dissipation energy maxima recorded during the rotational process (total rotated molecules = 47). (E–G) Proposed mechanism of the tip-induced rotation of the molecule.

tip, leading to either a decrease or an increase of the junction instability. Nevertheless, the significant dissipation peaks observed in Figure 4D obtained for the same oscillation amplitude clearly come from two different interactions of the CN groups with the surface in the saddle geometry while rotating the molecule. When the tip–molecule junction breaks, the CN end group interacting with the copper has laterally changed its position on the surface and the molecule thus re-adopts its saddle conformation with a 60° rotation with respect to its initial position (Figure 4G). Depending on the selected N atoms, the direction of the lateral displacement is reversed, which leads to inverted rotation directions.

CONCLUSION

In summary, we demonstrate a new route toward controlled manipulation of single molecules on surfaces. Using 3D spectroscopic measurements with sub-Ångström resolution, we chemically recognize specific carbonitrile functional groups within the porphyrin structure in the saddle conformation. We have also found that specific tip–molecule interactions at these locations allow the creation of a tip–molecule N···Cu coordination bond. This particularity has been used to apply external pulling forces to investigate the intrinsic elasticity of the molecule. Furthermore, we developed a reliable procedure to mechanically induce directed

molecular rotations. Spectroscopic measurements also provide direct information on the energy dissipated between the tip and the molecule involved in the manipulation process. Although the deformation due to the tip−molecule junction created within the manipulation process is purely elastic, we experimentally measured a significant dissipation energy value that we attribute to two different interactions of the CN end groups with the surface. The results emphasize the importance for fundamental studies of the mechanical properties and local chemical reactivity of complex molecular structures in order to better understand diffusive processes at the molecular scale. Such systematic studies might also open the way for mechanically driven manipulation techniques or local force-induced chemical reactions at the atomic scale.[43]

METHODS

Sample Preparation. The Cu(111) substrate was prepared inside the vacuum chamber with a base pressure lower than 5×10^{-10} mbar by repeated Ar^+ sputtering and subsequent annealing cycles (870 K). The porphyrin molecules were thermally evaporated from a quartz glass crucible being heated up to 535 K onto the Cu(111) substrate cooled at 80 K.

STM Experiments. STM experiments were performed with a commercial qPlus STM/AFM microscope (Omicron Nanotechnology GmbH) running at low temperature (5K) under ultrahigh vacuum lower than 1×10^{-10} mbar and operated by a Nanonis Control System from SPECS GmbH. We used a commercial tuning fork sensor in the qPlus configuration[42] (resonance frequency $f_0 \approx 26$ kHz, spring constant $k_0 \approx 1800$ N/m, typical quality factor $Q = 35\,000$ at 5 K). All STM images were recorded in the constant-current mode with the bias voltage applied to the tungsten tip. The tip was gently indented several times to the substrate before measurements to improve its quality and was thus terminated with copper adatoms.

Three-Dimensional Spectroscopic Measurement (3D-DFS). The frequency shift $\Delta f(z)$ and I_t *versus* distance z curves were recorded simultaneously above molecules at 5 K, in order to construct a box of 3.2 nm × 3.2 nm × 0.5 nm length containing 71 × 71 × 128 data points. The thermal drift during measurements was compensated by using atom-tracked positioning[40] before each distance-dependent measurement, and the bias voltage applied to the tip was set in the range of few microvolts. The oscillation amplitude was always set between 40 and 60 pm. Additionally, a $\Delta f(z)$ curve was taken (typical retraction distance ≈5−10 nm) after the complete spectroscopic measurement in order to estimate the long-range van der Waals background.

The dissipated energy per oscillation cycle E between the tip and the substrate has been extracted with the formula

$$E \approx \frac{\pi k A^2}{Q_0}\left[\frac{A_{exc} - A_{exc,0}}{A_{exc,0}}\right]$$

where k is the tuning fork stiffness, A the oscillation amplitude of the tip, Q_0 the intrinsic quality factor, and A_{exc} the excitation amplitude required to keep constant the oscillation amplitude of the tip in interaction with the sample.[44]

Conflict of Interest: The authors declare no competing financial interest.

Acknowledgment. We thank Pr. Edwin Constable for stimulating discussions. We acknowledge financial support from the Swiss National Science Foundation (NSF), the ESF EUROCORE program FANAS, and the Swiss National Center of Competence in Research on "Nanoscale Science" (NCCR-NANO).

REFERENCES AND NOTES

1. van Delden, R. A.; ter Wiel, M. K. J.; Pollard, M. M.; Vicario, J.; Koumura, N.; Feringa, B. L. Unidirectional Molecular Motor on a Gold Surface. *Nature* **2005**, *437*, 1337–1340.
2. Harikumar, K. R.; Polanyi, J. C.; Zabet-Khosousi, A.; Czekala, P.; Lin, H.; Hofer, W. A. Directed Long-Range Molecular Migration Energized by Surface Reaction. *Nat. Chem.* **2011**, *3*, 400–409.
3. Tierney, H. L.; Murphy, C. J.; Jewell, A. D.; Baber, A. E.; Iski, E. V.; Khodaverdian, H. Y.; McGuire, A. F.; Klebanov, N.; Sykes, E. C. H. Experimental Demonstration of a Single-Molecule Electric Motor. *Nat. Nanotechnol.* **2011**, *6*, 625–629.
4. Kudernac, T.; Ruangsupapichat, N.; Parschau, M.; Maciá, B.; Katsonis, N.; Harutyunyan, S. R.; Ernst, K.-H.; Feringa, B. L. Electrically Driven Directional Motion of a Four-Wheeled Molecule on a Surface. *Nature* **2011**, *479*, 208–211.
5. Grill, L.; Rieder, K.-H.; Moresco, F. Exploring the Interactomic Forces between a Tip and Single Molecules during STM Manipulation. *Nano Lett.* **2006**, *12*, 2685–2689.
6. Binnig, G.; Roher, H.; Gerber, C.; Weibel, E. Surface Studies by Scanning Tunneling Microscopy. *Phys. Rev. Lett.* **1982**, *49*, 57–61.
7. Binnig, G.; Quate, C.; Gerber, C. Atomic Force Microscope. *Phys. Rev. Lett.* **1986**, *56*, 930–933.
8. Eigler, D.; Schweizer, E. Positioning Single Atoms with a Scanning Tunnelling Microscope. *Nature* **1990**, *344*, 524–526.
9. Stroscio, J.; Celotta, R. Controlling the Dynamics of a Single Atom in Lateral Atom Manipulation. *Science* **2004**, *306*, 242–245.
10. Bartels, L.; Meyer, G.; Rieder, K.-H. Controlled Vertical Manipulation of Single CO Molecule with the Scanning Tunneling Microscope: A Route to Chemical Contrast. *Appl. Phys. Lett.* **1997**, *71*, 213–216.
11. Jung, T. A.; Schlittler, R.; Gimzewski, J.; Tang, H.; Joachim, C. Controlled Room-Temperature Positioning of Individuals Molecules: Molecular Flexure and Motion. *Science* **1996**, *271*, 181–184.
12. Moresco, F.; Meyer, G.; Rieder, K.-H.; Tang, H.; Gourdon, A.; Joachim, C. Conformational Changes of Single Molecule Induced by Scanning Tunnelling Microscopy Manipulation: A Route to Molecular Switching. *Phys. Rev. Lett.* **2001**, *86*, 672–677.
13. Grill, L. Large Molecules on Surfaces: Deposition and Intramolecular STM Manipulation by Directional Forces. *J. Phys.: Condens. Matter* **2010**, *22*, 084023-1–084023-14.
14. Giessibl, F. Atomic Resolution of the Silicon (111)-(7 × 7) Surface by Atomic Force Microscopy. *Science* **1995**, *267*, 68–71.
15. Pawlak, R.; Kawai, S.; Fremy, S.; Glatzel, T.; Meyer, E. Atomic-Scale Mechanical Properties of Orientated C_{60} Molecules Revealed by nc-AFM. *ACS Nano* **2011**, *5*, 6349–6354.
16. Sugimoto, Y.; Abe, M.; Hirayama, S.; Oyabu, N.; Custance, O.; Morita, S. Atom Inlays Performed at Room Temperature Using Atomic Force Microscopy. *Nat. Mater.* **2005**, *4*, 156–159.
17. Sugimoto, Y.; Pou, P.; Custance, O.; Jelinek, P.; Abe, M.; Perez, R.; Morita, S. Complex Patterning by Vertical Interchange Atom Manipulation Using Atomic Force Microscopy. *Science* **2008**, *322*, 413–417.
18. Ternes, M.; Lutz, C. P.; Hirjibehedin, C. F.; Giessibl, F. J. The Force Needed To Move an Adatom on a Surface. *Science* **2008**, *319*, 1066–1069.
19. Such, B.; Trevethan, T.; Glatzel, T.; Kawai, S.; Zimmerli, L.; Meyer, E.; Schluger, A. L.; Amijs, C. H. M.; de Mendoza, P.;

Echavarren, A. M. Functionalized Truxenes: Adsorption and Diffusion of Single Molecule on the KBr(001) Surface. *ACS Nano* **2010**, *4*, 3429–3439.
20. Loppacher, C.; Guggisberg, M.; Pfeiffer, O.; Meyer, E.; Bammerlin, M.; Lüthi, R.; Schlittler, R.; Gimzewski, J. K.; Tang, H.; Joachim, C. Direct Determination of the Energy Required To Operate a Single Molecule Switch. *Phys. Rev. Lett.* **2003**, *6*, 066107-1–066107-4.
21. Schütte, J.; Bechstein, R.; Rahe, P.; Langhals, H.; Rohlfing, M.; Kühnle, A. Single-Molecule Switching with Non-contact Atomic Force Microscopy. *Nanotechnology* **2011**, *22*, 245701-1–245701-6.
22. Sugimoto, Y.; Pou, P.; Abe, M.; Jelinek, J.; Pérez, R.; Morita, S.; Custance, O. Chemical Identification of Individual Surface Atoms by Atomic Force Microscopy. *Nature* **2007**, *446*, 64–67.
23. Meyer, E.; Glatzel, T. Novel Probes for Molecular Electronics. *Science* **2009**, *324*, 1397–1398.
24. Kawai, S.; Kawakatsu, H. Surface-Relaxation-Induced Giant Corrugation on Graphite(0001). *Phys. Rev. B* **2009**, *79*, 115440-1–115440-5.
25. Gross, L.; Mohn, F.; Moll, N.; Liljeroth, P.; Meyer, G. The Chemical Structure of a Molecule Resolved by Atomic Force Microscopy. *Science* **2009**, *325*, 1110–1114.
26. Mohn, F.; Repp, J.; Gross, L.; Meyer, G.; Dyer, M. S.; Persson, M. Reversible Bond Formation in a Gold-Atom Organic-Molecule Complex as a Molecular Switch. *Phys. Rev. Lett.* **2010**, *4*, 266102-1–266102-4.
27. Gross, L. Recent Advances in Submolecular Resolution with Scanning Probe Microscopy. *Nat. Chem.* **2011**, *3*, 273–278.
28. Pawlak, R.; Kawai, S.; Fremy, S.; Glatzel, T.; Meyer, E. High-Resolution Imaging of C_{60} Molecules Using Tuning-Fork-Based Non-contact Atomic Force Microscopy. *J. Phys.: Condens. Matter* **2012**, *24*, 084005-1–084005-10.
29. Fendt, L.-A.; Fang, H.; Plonska-Brzezinska, M. E.; Zhang, S.; Cheng, F.; Braun, C.; Echegoyen, L.; Diederich, F. Meso, Meso-Linked and Triply Fused Diporphyrins with Mixed-Metal Ions: Synthesis and Electrochemical Investigations. *Eur. J. Org. Chem.* **2007**, 4659–4673.
30. Marschall, M.; Reichert, J.; Weber-Bargioni, A.; Seufert, K.; Auwärter, W.; Klyatskaya, S.; Zoppellaro, G.; Ruben, M.; Barth, J. V. Random 2D String Networks Based on Divergent Coordination Assembly. *Nat. Chem.* **2010**, *2*, 131–137.
31. Yokoyama, T.; Yokoyama, S.; Kamikado, T.; Okuno, Y.; Mashiko, S. Selective Assembly on a Surface of Supramolecular Aggregates with Controlled Size and Shape. *Nature* **2001**, *413*, 619–621.
32. Tseng, T.-C.; Urban, C.; Wang, Y.; Otero, R.; Tait, S. L.; Alcamí, M.; Ecija, D.; Trelka, M.; Gallego, J. M.; Lin, N.; *et al.* Charge-Transfer-Induced Structural Rearrangements at Both Sides of Organic/Metal Interfaces. *Nat. Chem.* **2009**, *2*, 374–379.
33. Maier, S.; Fendt, L.-A.; Zimmerli, L.; Glatzel, G.; Pfeiffer, O.; Diederich, F.; Meyer, E. Nanoscale Engineering of Molecular Porphyrin Wires on Insulating Surfaces. *Small* **2008**, *8*, 1115–1118.
34. Glatzel, T.; Zimmerli, L.; Kawai, S.; Meyer, E.; Fendt, L.-A.; Diederich, F. Oriented Growth of Porphyrin-Based Molecular Wires on Ionic Crystals Analysed by NC-AFM. *Beilstein J. Nanotechnol.* **2011**, *2*, 34–39.
35. Trevethan, T.; Such, B.; Glatzel, T.; Kawai, T.; Schluger, A. L.; Meyer, E.; de Mendoza, P.; Echavarren, A. M. Organic Molecules Reconstruct Nanostructures on Ionic Surfaces. *Small* **2011**, *7*, 1264–1270.
36. Iancu, V.; Deshpande, A.; Hla, S.-W. Manipulating Kondo Temperature *via* Single Molecule Switching. *Nano Lett.* **2006**, *6*, 820–823.
37. Moresco, F.; Meyer, G.; Rieder, K.-H.; Ping, J.; Tang, H.; Joachim, C. TBPP Molecules on Copper Surfaces: A Low Temperature Scanning Tunneling Microscope Investigation. *Surf. Sci.* **2002**, *499*, 94–102.
38. Lafferentz, L.; Ample, F.; Yu, H.; Hecht, S.; Joachim, C.; Grill, L. Conductance of a Single Conjugated Polymer as a Continuous Function of Its Length. *Science* **2009**, *323*, 1193–1197.
39. Fournier, N.; Wagner, C.; Weiss, C.; Temirov, R.; Tautz, F. S. Force-Controlled Lifting of Molecular Wires. *Phys. Rev. B* **2011**, *84*, 035435-1–035435-5.
40. Kawai, S.; Glatzel, T.; Koch, S.; Baratoff, A.; Meyer, E. Interaction-Induced Atomic Displacements Revealed by Drift-Corrected Dynamic Force Spectroscopy. *Phys. Rev. B* **2011**, *3*, 035421-1–035421-7.
41. Kawai, S.; Canova, F. F.; Glatzel, T.; Foster, A. S.; Meyer, E. Atomic-Scale Dissipation Processes in Dynamic Force Spectroscopy. *Phys. Rev. B* **2011**, *84*, 115415-1–115415-9.
42. Giessibl, F. Atomic Resolution on Si(111)-(7 × 7) by Non-contact Atomic Force Microscopy with a Force Sensor Based on a Quartz Tuning Fork. *Appl. Phys. Lett.* **2000**, *76*, 1470–1472.
43. Davis, D. A.; Hamilton, A.; Yang, J.; Cremar, L. D.; Van Gough, D.; Potisek, S. L.; Ong, M. T.; Braun, P. V.; Martínez, T. J.; White, S. R.; *et al.* Force-Induced Activation of Covalent Bonds in Mechanoresponsive Polymeric Materials. *Nature* **2009**, *459*, 68–72.
44. Anczyowski, B.; Gotsmann, B.; Fuchs, H.; Cleveland, J. P.; Elings, V. B. How To Measure Dissipation in Dynamic Mode Atomic Force Microscopy. *Appl. Surf. Sci.* **1999**, *140*, 376–382.